Pharmacokinetics and Biodistribution of a Nucleotide-Based Thrombin Inhibitor in Rats

Larisa Reyderman[1] and Salomon Stavchansky[1,2]

Received December 23, 1997; accepted March 21, 1998

Purpose. To characterize the pharmacokinetic and tissue distribution profiles of a nucleotide-based thrombin inhibitor (GS522, phosphodiester oligonucleotide, GGTTGGTGTGGTTGG) following intravenous administration to rats.

Methods. *Pharmacokinetic study:* 10 mg/kg, 20 mg/kg, 30 mg/kg (6 animals/dose) were administered to rats by rapid injection into the femoral vein. Blood samples were collected over a 45 minute period. Plasma concentrations of GS522 were determined using capillary gel electrophoresis with laser-induced fluorescence detection. *Biodistribution Study:* 10mg/kg (400μl, 31.46 μCi/ml) of ^{3}H-GS522 was administered to rats by rapid injection into the femoral vein. The animals were sacrificed by decapitation at 1, 5, 10, 30, 60, 360 minutes post-dose (3 rats/point). Brain, blood, duodenum, eyes, heart, kidney, liver, lungs, muscle, pancreas, skin, spleen and vein samples were collected, processed and quantitated using liquid scintillation counting.

Results. The pharmacokinetic profile declines in multiexponential manner, exhibiting extremely fast distribution and elimination ($t_{1/2}$ = 7.6–9.0 min, Cl = 22.0–28.0 ml/min, V = 83.9–132.4 ml/kg). GS522 follows linear pharmacokinetics, with the area under the curve being proportional to the dose (Rsq = 0.9744). Highest radioactivity levels were detected in kidney, liver and blood (39.7, 15.7 and 15.3% dose/respective organ). Less than 1% of the dose was detected in the heart, spleen and lungs, and >0.3% of the dose was found in the brain and eyes. The oligonucleotide associated radioactivity was uniformly distributed between the brain regions (left and right lobe and cerebellum). Six hours following the dose administration a statistically significant increase ($p < 0.05$) in radioactivity levels was observed in the brain, eyes, skin, liver, pancreas and vein.

Conclusions. The pharmacokinetic and biodistribution profiles of GS522 following intravenous administration to rats at three doses were characterized. The oligonucleotide associated radioactivity was widely distributed in tissues. The amount of radioactivity sharply decreased with time in most tissues. Kidney, liver and muscle were the main sites of accumulation. The oligonucleotide associated radioactivity did not cross the blood brain barrier to an appreciable extent. In addition, a statistically significant increase ($p < 0.05$) in the radioactivity levels observed in select tissues suggested a re-uptake mechanism for intact oligonucleotide or its degradation products.

KEY WORDS: GS522; oligodeoxynucleotide; pharmacokinetics; tritiated; biodistribution; rat.

INTRODUCTION

The last decade have seen the evolution of novel therapeutic strategies, one of them being the so-called "informational" drugs. Informational drugs are nucleic acid polymers capable of interfering with major functions of proteins or nucleic acids encoding these proteins. Classification of the informational drugs is performed based on their mechanism of action. Antisense therapy relies on the hybridization of an oligonucleotide to the "sense" messenger RNA (mRNA) in a sequence specific manner to inhibit gene expression, i.e. production of the target protein. Triplex helix forming oligonucleotides bind to specific regions of the dsDNA disrupting RNA transcription from a gene by sterically blocking recognition by transcription factors. Additionally, oligonucleotides can be designed to specifically bind proteins that perform regulatory functions or are involved in the regulation of the genes.

GS522 is a novel oligodeoxynucleotide, GGTTGGTGT GGTTGG, that has specific inhibitory activity toward thrombin (1). *In vitro* studies have shown GS522 to be capable of nanomolar (2.7 nM) inhibition of thrombus cleavage, clot-bound thrombin inhibition and reduction of the arterial thrombus formation in an *ex vivo* whole artery angioplasty model (2). The pharmacological studies conducted in cynomongolus monkeys and dogs proved GS522 to possess *in vivo* anticoagulant properties with an extremely short half life (3, 4). Short half-life of the thrombin aptamer makes it an advantageous anticoagulant agent in cardiopulmonary bypass, since it allows for the rapid reversal of anticoagulation with no need for specific antagonist.

The purpose of this investigation is to describe the pharmacokinetics and biodistribution of GS522 in rats following intravenous administration to rats.

MATERIALS AND METHODS

Formulations

Pharmacokinetic Study

The solution of GS522 used for intravenous administration was prepared by dissolving 25 mg of GS522 in 5 ml of PBS (phosphate buffered saline, pH = 7.4). The resulting solution (5 mg/ml) was filtered through a 0.2 μm filter. Approximately 0.5 ml of this solution was administered to the rats via the femoral vein.

Biodistribution Study

GS522 oligonucleotide was radiolabeled by Moravek Biochemicals (La Brea, CA) according to the tritium exchange procedure reported by Lesnik et al. (5). The characterization of the GS522 solution following the radiolabeling procedure was conducted in our laboratories and included the scintillation counting, UV scan, and triplicate measurement of the absorbance of a 10 μl aliquot.

A solution of GS522 used for intravenous administration was prepared by adding 0.75 ml (8.9 mg) of $_3$H-GS522 (421.9 μCi/ml, 35.5 μCi/mg) to 41.41 mg of GS522 following dissolution in 10 ml of 0.9% saline to yield a final concentration of 5.0 mg/ml. The specific activity of the GS522 solution (31.5 μCi/ml) was determined by scintillation counting of three 10 μl aliquots in 5 ml of Ready Value scintillation cocktail (700000 ± 19000 dpm/10 μl). The dose (400 μl) was carefully weighed in the syringe to minimize the variability of the amount of GS522 administered to the rat.

[1] The University of Texas at Austin, College of Pharmacy, PHR 4.214C, Division of Pharmaceutics, Austin, Texas 78712.

[2] To whom correspondence should be addressed. (e-mail: stavchansky@mail.utexas.edu)

0724-8741/98/0600-0904$15.00/0

Animals

Male Sprague Dawley rats weighing 200–250 grams were used for the study. The rats were purchased from the Harlan Laboratories (Indianapolis, IN). A total of 18 rats (3 per each time point) were used to study the biodistribution of the radiolabeled oligonucleotide. Additionally, 18 rats were used for the pharmacokinetic studies (6 per each dose). The rats were acclimated for 1 week prior to surgery, and fasted 12 hours prior to surgery. During this time, water was allowed *ad libitum.*

Experimental Procedure

The experimental protocol was approved by the Animal Resource Center of the University of Texas at Austin, and conformed with current NIH/PHS and USDA guidelines and regulations. Each animal was weighed and anesthetized intraperitoneally with 0.6 ml/kg of rodent anesthesia cocktail (ketamine HCL 42.86%, xylazine HCL 20%, acepromazine 10%).

Pharmacokinetics Study

Approximately 0.5 ml of GS522 (oligo) solution was administered over a 30 second period via a polyethylene cannula (PE-50 tubing) inserted into the femoral vein. The volume of the administered dose was adjusted according to the weight of the animal to deliver 10 mg/kg, 20 mg/kg or 30 mg/kg dose (6 rats per dose). The cannula was immediately flushed with isotonic saline solution after each injection to ensure complete oligonucleotide delivery. Blood samples (300 μl) were collected at 0 (pre-dose), and at 1, 2, 5, 7, 10, 20, 30, 45 minutes post administration. The blood samples were immediately transferred to citrated tubes (1:10, 3.2% sodium citrate to blood) and placed on chipped ice. Plasma was harvested by centrifugation for one minute at 10,000 *g* at 4°C and stored at −20°C until analyzed.

Biodistribution Study

Four hundred microliters (400μl) of GS522 was administered into the femoral vein over a 30 seconds time interval. The cannula was immediately flushed with isotonic saline solution (300μl) to ensure complete oligonucleotide delivery. The animals were sacrificed by decapitation at 1, 5, 10, 30, 60, 360 minutes post-dose. Three animals were used at each time point. Brain, duodenum, eyes, heart, kidney, liver, lungs, muscle, pancreas, skin, spleen and vein were excised, thoroughly washed with saline solution, weighed, and flash frozen in liquid nitrogen. Blood samples were drawn into heparinized tubes (Vacutainers) immediately after the decapitation step. In order to prevent oligonucleotide decomposition, blood aliquots were immediately processed and plasma separated by centrifugation at 10,000 *g* for 2 minutes at 4°C.

Sample Preparation

Pharmacokinetic Study

Plasma samples analyzed for GS522 and its potential metabolites using a validated capillary gel electrophoresis method (6). Detection was by laser-induced fluorescence at 485 and 520 nm excitation and emission wavelength, respectively. The method was linear over the range 20 ng/ml to 1520 ng/ml and the limit of quantitation was set to 20 ng/ml. In some instances, the plasma samples were diluted 1:10 with de-ionized water with the purpose of ensuring that the concentration of GS522 in plasma was within the linear dynamic range of the assay.

Biodistribution Study

Approximately 100 mg of each collected tissue was weighed and added to a liquid scintillation vial containing 1 ml of tissue solubilizer (Beckman, Fullerton, CA). Samples were digested overnight at 55°C in a shaker bath. Decolorization of samples was accomplished by adding 100μl of 30% hydrogen peroxide (H_2O_2) (EM Science, Gibbstown, NJ). After incubation for 30 minutes at 55°C, chemiluminescence was reduced by the addition of 50μl of glacial acetic acid (MCB reagents, Cincinnati, OH). ReadyOrganic liquid scintillation cocktail (Beckman Instruments, Fullerton, CA) (5ml) was added to all samples, which were then counted with a Beckman LS 6000 Liquid Scintillation Counter (Beckman Instruments, Fullerton, CA).

Blood samples for scintillation counting were prepared by adding 0.7ml of tissue solubilizer-isopropanol mixture (1:2 v/v) to 100μl of blood. The samples were then incubated overnight (approximately 10 hr) at 55°C. Three hundred microliters (300μl) of H_2O_2 were added to the samples and incubated for an additional 30 minute period at 55°C. The samples were then counted in 5 ml of ReadyOrganic scintillation cocktail (Beckman Instruments, Fullerton, CA) containing 50μl of glacial acetic acid.

Quench Calibration Curves

Quench curves for each tissue or organ sample were constructed with the purpose of estimating the counting efficiencies. Three samples of approximately 75 mg, 100 mg, 120 mg of each tissue obtained from the control rat were spiked with a known amount of radioactivity (10μl of 0.42 mCi/ml stock solution). These samples were submitted to the same sample treatment procedure and radioactivity was determined by scintillation counting. Three vials containing the aliquots of ^{3}H-GS522 added to each tissue sample (10μl of 0.42 mCi/ml stock solution) were counted in 5 ml ReadyValue cocktail to determine the "true" counts per minute value. The counting efficiency of each tissue sample was calculated dividing counts per minutes of each sample by the "true" counts per minute of the known amount of radioactivity added to each tissue.

To determine the counting efficiency of the eyes, two samples (one eye each sample) were prepared and radioactivity was determined by scintillation counting. The average efficiency of these two samples were used in the calculation of experimental results.

Data Analysis

Pharmacokinetic Study

Noncompartmental analysis of the data was performed (WINNONLIN, Version 1.1). The area under the plasma concentration time curve was calculated using the trapezoidal rule for the observed values and the extrapolation to infinity. The

elimination half-life was estimated from the terminal linear segment of the plasma concentration curve. In addition, the plasma concentration time profiles were fited to a two-compartment model to determine the rate constants k_{10}, k_{12}, k_{21} associated with the elimination of drug from plasma and drug transfer between plasma and tissue compartments, respectively.

Biodistribution Study

Data were calculated as percentage of Dose/organ and percentage of Dose/gram of tissue. The rate of disappearance of the oligonucleotide associated radioactivity from the tissues was determined based on the monoexponential equation (WINNONLIN, Version 1.1)

$$C(t) = A \cdot \exp(-k \cdot t) \quad (1)$$

where, C_t is the concentration of radioactivity at time t, A_i is the extrapolated initial amount of radioactivity, k is the elimination rate constant (1/min).

Radioactivity time profile of the blood was described based on the bi-exponential modeling.

$$C(t) = Ae^{-\alpha t} + Be^{-\beta t} \quad (2)$$

where A, B (μg/ml), α, β (1/min) are coefficients and macro constants determined by curve stripping.

RESULTS

Pharmacokinetics

The plasma concentration time profiles obtained following intravenous bolus administration of 10 mg/kg, 20 mg/kg and 30 mg/kg of GS522 to rats are shown in Figure 1. The plasma concentration of GS522 declines in an exponential fashion, suggesting a first order process. The plasma concentration of GS522 during the elimination phase is similar at all three doses studied. The distribution phase of GS522 is extremely fast. This rapid decline in the plasma concentration of GS522 may have contributed to the variability observed during the first 2 minutes post-administration. The pharmacokinetic parameters obtained by noncompartmental modeling are summarized in Table 1. The volume of distribution at steady state was 115.09 ml/kg, 83.86 ml/kg and 132.40 ml/kg for the three administered doses, which indicates a wide GS522 distribution. The elimination phase associated half-life of 7.6–9.0 minutes indicates rapid disappearance of the drug from the systemic circulation.

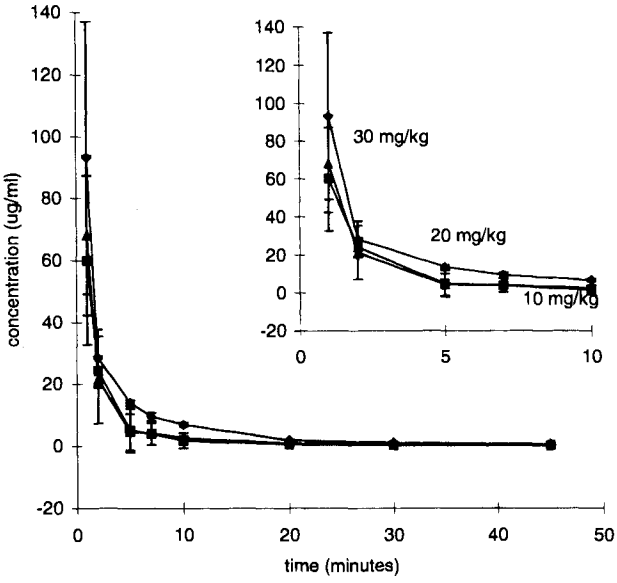

Fig. 1. Pharmacokinetic profile of GS522 following intravenous administration to rats.

The AUC and C_o values of the three doses indicate an apparent dose-proportionality (Figure 3). In a statistical sense, a linear drug disposition means that the drug molecules act independently of other molecules in their elimination and distribution behavior. The slope of the AUC vs *Dose* plot is equal to the inverse of clearance. The clearance value obtained based on the plot (20.2 ml/min) is in agreement with that estimated by the noncompartmental modeling of the data (23.0 ml/min, 22.0 ml/min, 28.0 ml/min for 10 mg/kg, 20 mg/kg, 30 mg/kg doses, respectively).

Biodistribution

The biodistribution data generated after intravenous bolus injection of ^{3}H-GS522 is shown in Table 2. The results indicate that the radiolabel undergoes a wide tissue distribution (Figure 4). Higher radioactivity levels were detected in kidney, liver and blood. One minute following dose administration the highest radioactivity levels, 22.3% and 15.7% of the dose, were detected in the kidneys and liver, respectively. The total recovery 1 minute after injection was 57.3% of the dose. Less than 1% of the dose was detected in the heart, spleen and lungs, and > 0.3% of the dose was found in the brain and eyes. The amount of radioactivity sharply decreased with time in most tissues. One hour following dose administration only 0.8% of the dose was detected in the blood, compared to 15.1% at 1 minute. A total of 13.8% of the total radioactivity of the dose was detected in the animals at 6 hours.

Figure 5 shows the biodistribution of the oligonucleotide associated radioactivity in the brain. The results of the study indicate that the radiolabel is uniformly distributed in the brain. The kinetics of the distribution is similar in the cerebellum and the left and right lobes of the brain. A statistically significant increase ($p < 0.05$) in the radioactivity levels 6 hr after the dosage administration is detected in the brain segments. Radiolabel accumulation at later time points in the brain was also reported following intravenous administration of the chimeric phosphorothioate oligonucleotide in rats (7). A statistically significant increase ($p < 0.05$) in the radioactivity levels 6 hr post dose was observed in the brain, eyes, liver, lungs, pancreas and vein.

DISCUSSION

Figure 2 shows typical electropherograms obtained 1 and 2 minutes following dose administration. Two interesting features of these electropherograms: 1) drastic decrease of the GS522 peak height indicate fast drug disappearance from plasma, and 2) the presence of distinct small peaks prior to GS522 peak (Figure 2 insets).

The CGE with LIF detection method developed for the quantitation of ss-oligos (6) relies on high affinity binding of

Table 1. Pharmacokinetic Parameters of GS522 Following Intravenous Administration to Rats (Mean ± SD)

Parameter	Dose 10 mg/kg	Dose 20 mg/kg	Dose 30 mg/kg
C_o (μg/ml/kg)	317.8 ± 154.0	558.4 ± 163.3	1274.3 ± 1296.1
k (1/min)	0.09 ± 0.02	0.1 ± 0.04	0.08 ± 0.02
$t_{1/2}$ (min)	8.6 ± 2.4	7.6 ± 2.4	9.0 ± 2.4
v (ml/kg)	294.2 ± 118.9	261.2 ± 189.4	342.3 ± 182.4
$AUC_{o\to\infty}$ (μ ml/min/kg)	449.6 ± 108.8	1027.1 ± 387.0	1437.7 ± 993.3
Cl (ml/min)	23.0 ± 4.3	22.0 ± 9.1	28.0 ± 16.2
$AUMC_{o\to\infty}$ (μg ml/min^2/kg)	2093.8 ± 303.7	2985.3 ± 642.8	4454.8 ± 1261.5
$MRT_{o\to\infty}$ (min)	4.9 ± 1.2	3.3 ± 1.7	3.9 ± 2.3
Vss (ml/kg)	115.1 ± 39.3	83.9 ± 79.0	132.4 ± 137.0

the OliGreen™ reagent to ss-oligos. This property ensures that the peaks observed during the electrophoretic separations are those pertaining only to oligonucleotides. The presence of peaks prior to that of GS522 points to the presence of short oligo fragments generated via degradation of GS522 in plasma by nucleases. These fragments were observed for up to 7 minutes following the administration of the dose, after which time their concentration was probably lower than the limit of quantitation of the assay.

Fast disappearance of GS522 from plasma observed in the electropherograms is confirmed by high clearance values (22.0–27.8 ml/min). The elimination of GS522 from plasma can be attributed to fast digestion of the later by nucleases as well as the distribution to the tissues.

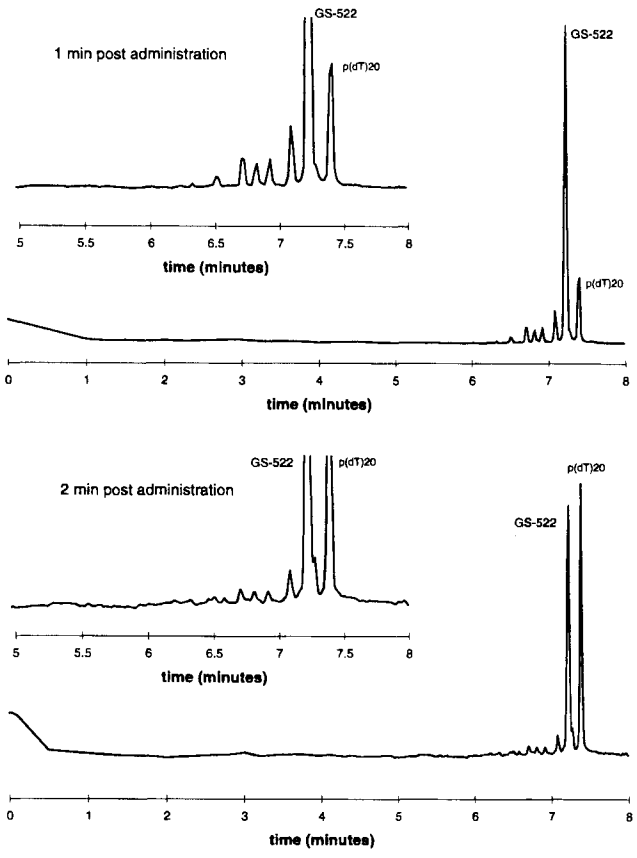

Fig. 2. Representative electropherograms obtained one and two minutes post intravenous administration of GS522 (10 mg/kg).

Based on the bi-exponential modeling of the data, the rate of elimination of GS522 from plasma (k_{10} = 0.92 - 1.26 1/min) is almost 3 times higher than the rates of transfer between the tissues (k_{12} = 0.36 - 0.48 1/min, and k_{21} = 0.15 - 0.19 1/min). This indicates, that disappearance of GS522 from plasma can be mostly attributed to the degradation by nucleases. These results are in agreement with the reports in the literature (8,9) on the instability of the phosphodiester oligos in plasma and *in vivo* due to susceptibility to nuclease digestion. In addition, the rate of transfer of GS522 to the tissues is approximately twice that of the opposing process, i.e. transfer from tissues back to plasma.

The biodistribution study was performed to further elucidate the pathways of disappearance of GS522 and its degradation products from plasma and their distribution in the tissues. The biodistribution studies of the phosphodiester oligonucleotides reported in the literature utilized enzymatic ^{32}P 5′ or 3′ end labeled oligonucleotides (10,11). Considering that the degradation of oligonucleotides in blood proceeds primarily via a 3′ as well as 5′ exonucleatic mechanism (8,12–16). The results of the biodistribution study of the end labeled molecule will not be an accurate representation of the distribution of the bulk of the oligonucleotide. For the purpose of this study GS522 was uniformly radiolabeled via hydrogen exchange between tritiated water and C8 position of purines at elevated temperature (90°C) (5). Compounds radiolabeled by this procedure exhibited greater than 90% of the specific activity following 72 hour incubation in physiological solutions (Dulbecco's Modified Eagle's Media containing 10% heat inactivated fetal bovine serum). The persistence of the radiolabel on the compound, i.e. lack of the radiolabel exchange between the medium and/or tissues and the compound is of utmost importance for the reliability of the results of biodistribution studies. The extended stability of the tritiated oligonucleotide under physiological conditions makes this labeling procedure appropriate for the present investigation.

The results of the study indicate that the oligonucleotide associated radioactivity is cleared rapidly from blood. Disappearance of the oligonucleotide associated radioactivity from blood was described by a sum of two exponentials (Figure 7). Estimates of steady state volumes of distribution and elimination half-life are 28.3 ml and 27.8 min, respectively. These values account for the intact oligonucleotide as well as the degradation products.

A rapid and substantial distribution of the radioactivity from blood into tissue was observed. The time course of the

Table 2. Biodistribution and Elimination ($T_{1/2}$) of ^{3}H-GS522 in Rats

	1 min	5 min	10 min	30 min	60 min	360 min	$T_{1/2}$ (min)
			% Dose/organ or tissue				
Blood	15.13 ± 3.66	9.94 ± 0.42	3.04 ± 0.78	2.00 ± 0.93	0.76 ± 0.03	0.51 ± 0.09	
Brain	0.14 ± 0.02	0.26 ± 0.05	0.21 ± 0.03	0.14 ± 0.03	0.09 ± 0.02	0.14 ± 0.02	37.37 ± 9.45
Eyes	0.03 ± 0.001	0.04 ± 0.001	0.04 ± 0.01	0.03 ± 0.003	0.02 ± 0.001	0.03 ± 0.01	61.68 ± 11.88
Heart	0.90 ± 0.17	0.58 ± 0.09	0.43 ± 0.09	0.21 ± 0.03	0.13 ± 0.03	0.13 ± 0.03	30.84 ± 6.95
Kidney	22.28 ± 3.61	39.69 ± 10.36	8.07 ± 0.47	6.51 ± 0.77	5.83 ± 1.32	2.86 ± 0.53	221.19 ± 66.49
Liver	15.66 ± 1.10	12.43 ± 2.52	9.85 ± 3.43	6.32 ± 2.06	3.72 ± 0.32	5.75 ± 1.28	40.20 ± 13.63
Lungs	0.46 ± 0.06	0.82 ± 0.10	0.55 ± 0.06	0.23 ± 0.03	0.22 ± 0.04	0.23 ± 0.01	35.07 ± 6.71
Muscle	2.25 ± 0.17	4.94 ± 0.31	3.59 ± 0.79	3.45 ± 0.67	1.58 ± 0.37	4.04 ± 0.02	61.53 ± 34.74
Spleen	0.43 ± 0.08	0.74 ± 0.24	0.37 ± 0.001	0.17 ± 0.01	0.24 ± 0.06	0.30 ± 0.22	21.42 ± 8.09
Amount recovered*	57.3%	69.4%	26.2%	19.1%	12.6%	14.0%	

* Calculated as the sum of the %Dose/organ values.

^{3}H-GS522 in the brain, eyes and muscle exhibited fast initial accumulation, with the oligonucleotide associated radioactivity reaching maximum in 4.5–5.7 minute. The uptake of the oligonucleotide associated radioactivity in such highly perfused tissues as heart, liver and lungs was almost instantaneous with maximum levels observed 1 minute post dose. The half-life of the elimination of the oligonucleotide associated radioactivity from the organs is summarized in Table 2. The slowest elimination of the oligonucleotide associated radioactivity with the half-life of 221.2 min was from the kidney.

Kidney and liver are the major sites of antisense oligonucleotide degradation, with kidney playing the major role in oligonucleotide elimination. Biodistribution studies of phosphorothioate antisense oligonucleotides in rats and mice have shown liver and kidney to be the predominant organs of accumulation (12,11,17). The concentration of the oligonucleotide associated radioactivity in liver was next highest to that in kidney (13,17). The accumulation of phosphorothioate oligonucleotides in the kidney was suggested to be mediated by a transport mechanism involving specific binding of the nucleic acid to the renal epithelium (18). A putative cell surface oligonucleotide receptors were identified from enriched brush border membrane preparations to be 46kDa and 97kDa proteins. Renal proximal tubule cells were theoreticized to have either cell type-specific nucleic acid receptors or have a general receptor for DNA. Kinetic studies of the renal uptake of an 18-mer phosphorothioate oligonucleotide showed extensive reabsorption of the oligo and its degradation products in the nephron (19). Oligonucleotides are hypothesized to be filtered by the glomerulus followed by the reuptake from the tubule lumen to the proximal tube.

In this investigation, the accumulation of the oligonucleotide and its degradation products in the tissues was determined based on the organ to blood ratio (Figure 6). A ratio of 1:1 or less observed in the brain, eyes, heart, lungs and spleen is indicative of the compound being freely diffusible without binding to or accumulating within these tissues. Organ to blood ratios of approximately 1:11, 1:8 and 1:7.7 for liver, muscle and kidney suggest that these organs may be the sites of accumulation of either oligonucleotide or, more likely, its degradation products. The results are in agreement with the distribution and accumulation profiles of oligonucleotides reported in the literature. Further studies will be required to determine the mechanisms of accumulation and possible reuptake of oligonucleotides and their degradation products in these organs.

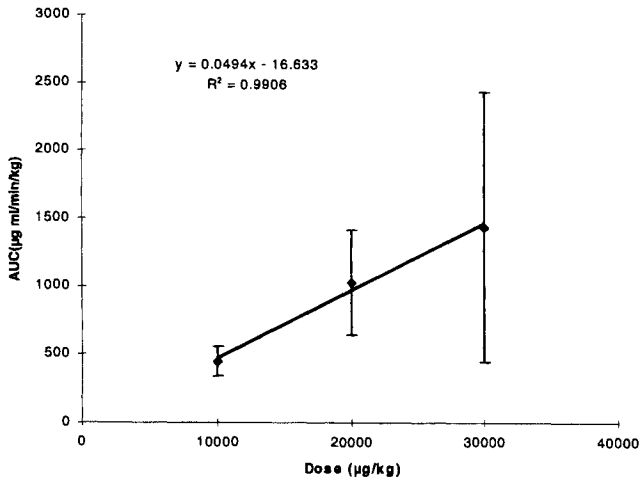

Fig. 3. Dose proportionality of the GS522 (Rsq = 0.99, F = 105.2). The slope of the line is equal to the reciprocal of the clearance (*CL* = 20.2 ml/min).

CONCLUSIONS

In conclusion, the pharmacokinetics of GS522 following intravenous administration of 10 mg/kg, 20 mg/kg or 30 mg/kg dose of GS522 to rats was characterized. The pharmacokinetic profile declines in a multiexponential manner, exhibiting extremely fast distribution and elimination ($t_{1/2}$ = 7.63-9.02 min). GS522 follows linear pharmacokinetics, with the area under the plasma concentration time curve being proportional to the administered dose (Rsq = 0.9744).

Rates of elimination of GS522 from plasma and exchange between plasma and tissues obtained through bi-exponential modeling of the data (k_{10} = 0.92–1.26 1/min, k_{12} = 0.36–0.48 1/min, and k_{21} = 0.15–0.19 1/min) indicate that: 1) fast disappearance of GS522 from plasma can be possibly attributed to digestion by nucleases, 2) GS522 has greater affinity for tissue compared to that for plasma. Rapid disappearance of GS522 from plasma and wide distribution into tissues is further indicated by values of clearance and volume of distribution (*CL* = 22.0–28.0 ml/min, *V* = 83.9–132.4 ml/kg).

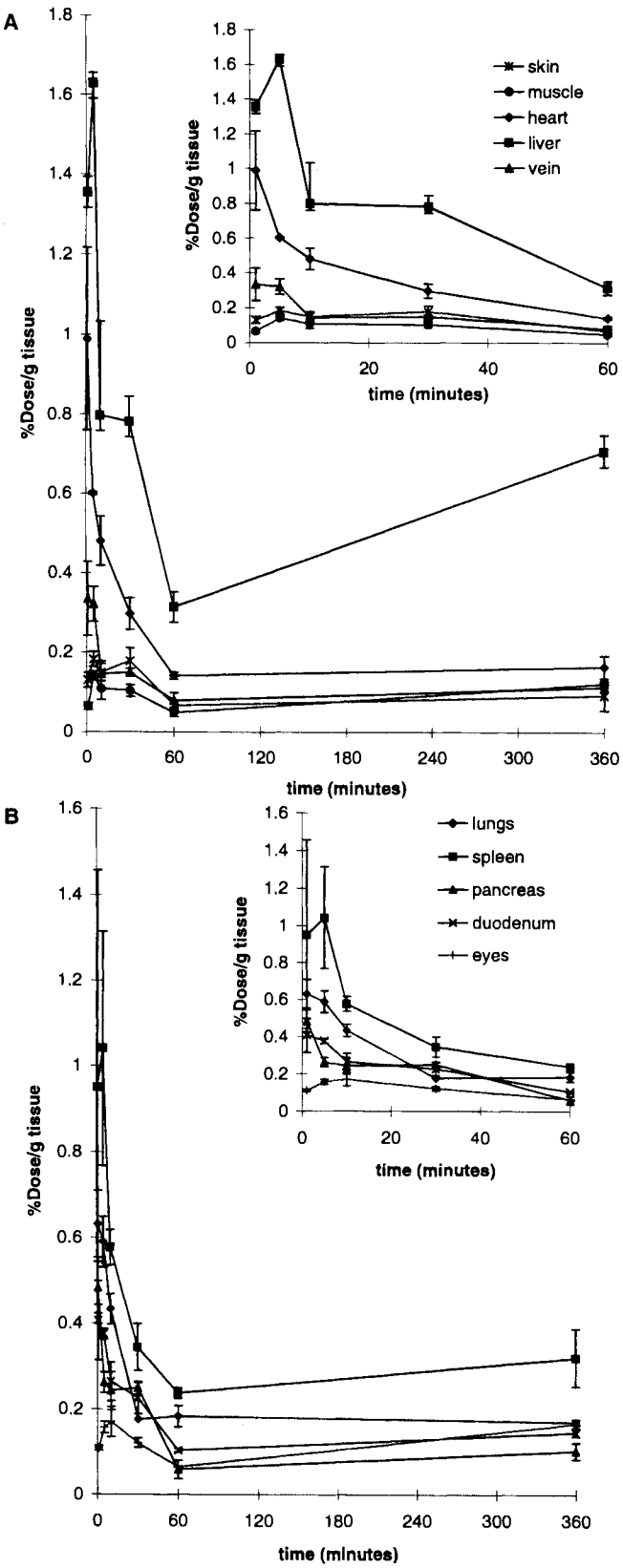

Fig. 4(A, B). Biodistribution of ^{3}H-GS522 in rat tissues after intravenous administration of 10 mg/kg of GS522 (n = 3).

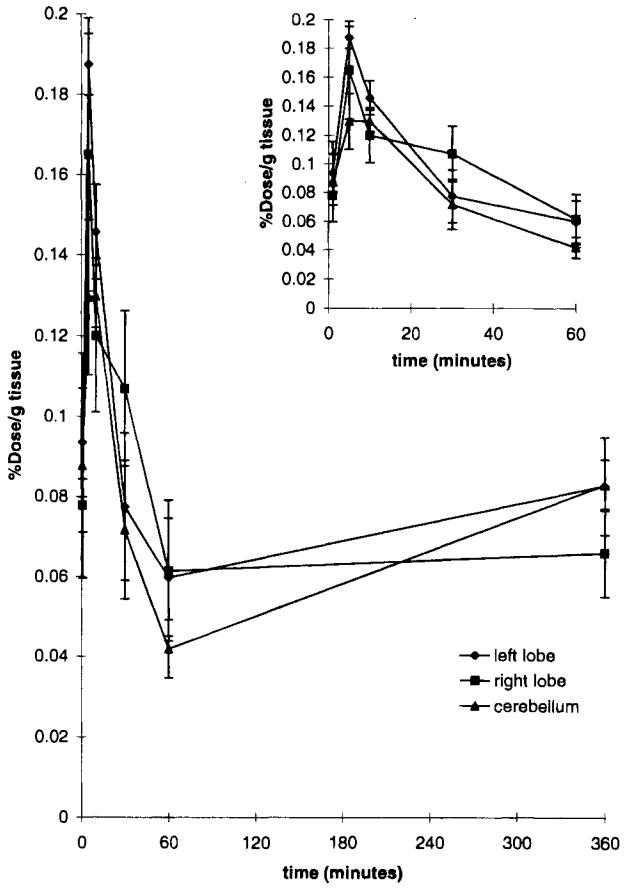

Fig. 5. Biodistribution of ^{3}H-GS522 in the brain following intravenous administration of 10 mg/kg (n = 3).

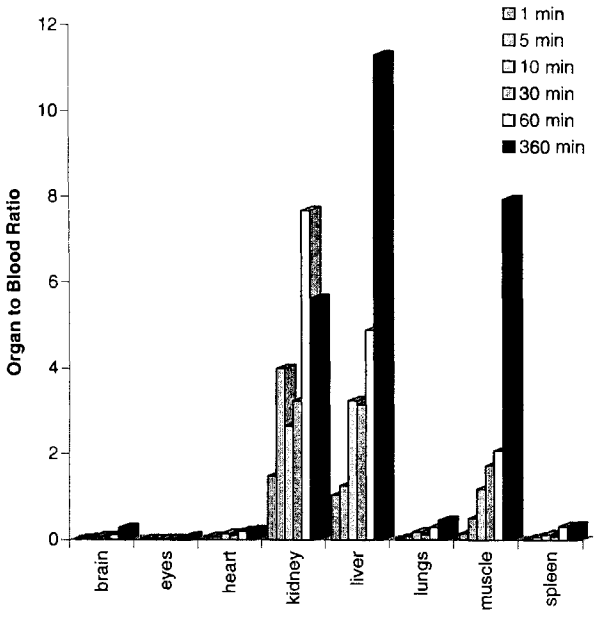

Fig. 6. Accumulation of ^{3}H-GS522 associated radioactivity in rat tissues following intravenous administration of 10 mg/kg.

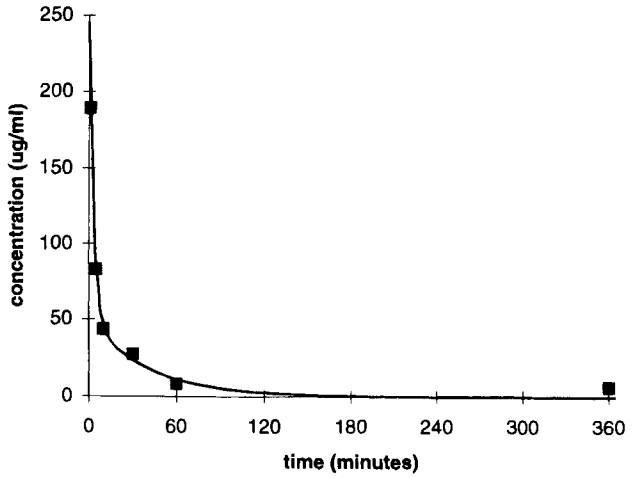

Fig. 7. Pharmacokinetic modeling of the radioactivity levels in blood.

The biodistribution study of the tritiated GS522 was investigated following 10 mg/kg intravenous bolus administration to rats. The results of the study indicate that the oligonucleotide associated radioactivity is widely distributed in tissues. The amount of radioactivity sharply decreases with time in most tissues. Highest radioactivity levels were detected in the kidneys and liver. Kidney, liver and muscle are the main sites of accumulation. The distribution of the radiolabel in three distinct brain regions (left and right lobes and cerebellum) was studied. The results indicate that the radiolabel is uniformly distributed between the brain regions. The oligonucleotide derived radioactivity does not cross the blood brain barrier to appreciable extent. A total of only 0.26% of the dose was detected in the brain. However, 6 hr following the dose administration a statistically significant increase in radioactivity levels was observed in the brain, eyes, skin, liver, pancreas and vein. These results alert to the potential toxicity due to the reuptake of oligonucleotide degradation products in these tissues.

ACKNOWLEDGMENTS

The authors would like to thank Dr. William Lee of Gilead Sciences, Inc. for the generous gift of GS-522 (15-mer ss-oligonucleotide).

REFERENCES

1. L. C. Griffin, G. F. Tidmarsh, L. C. Bock, J. J. Toole, and L. L. K. Leung. In vivo Anticoagulant Properties of a Novel Nucleotide-Based Thrombin Inhibitor and Demonstration of Regional Anticoagulation in Extracorporeal Circuits. *Blood* **81**:3271 (1993).
2. W.-X. Li, A. V. Kaplan, G. W. Grant, J. J. Toole, and L. K. Leug. A Novel Nucleotide-Based Thrombin Inhibitor Inhibits Clot-Bound Thrombin and Reduces Arterial Platelet Thrombus Formation. *Blood* **83**:677 (1994).
3. A. DeAnda, S. E. Coutre, M. R. Moon, C. N. Vial, L. C. Griffin, V. S. Law, M. Komeda, L. L. K. Leung, and D. C. Miler. Pilot Study of the Efficacy of a Thrombin Inhibitor for Use During Cardiopulmonary Bypass. *Ann. Thorac. Surg.* **58**:344 (1994).
4. W. A. Lee, J. A. Fishback, J-P. Shaw, L. C. Bock, L. C. Griffin, and K. C. Cundy. A Novel Oligonucleotide Inhibitor of Thrombin. II Pharmacokinetics in the Cynomolgus Monkey. *Pharm. Res.* **12**:1943 (1995).
5. M. J. Graham, S. M. Freier, R. M. Crooke, D. J. Ecker, R. N. Maslova, and E. A. Lesnik. Tritium Labeling of Antisense Oligonucleotides by Exchange with Tritiated Water. *Nucl. Acids Res.* **21**:3737 (1993).
6. L. Reyderman and S. Stavchansky. Quantitative Determination of Short Single-stranded Oligonucleotides From Blood Plasma Using Capillary Electrophoresis With Laser Induced Fluorescence. *Anal.Chem.*, in print (1997).
7. R. Zhang, R. P. Iyer, D. Yu, W. Tan, X. Zhang, Z. Lu, H. Zhqo, and S. Agrawal. Pharmacokinetics and Tissue Disposition of a Chimeric Oligodeoxynucleoside Phosphorothioate in Rats After Intravenous Administration. *J. Pharm. Exp. Ther.* **278**:971 (1996).
8. P. S. Eder, R. J. DeVine, J. M. Dagle, and J. A. Walder. Substrate Specificity and Kinetics of Degradation of Antisense Oligonucleotides by a 3'Exonuclease in Plasma. *Antisense Res. Develop.* **1**:141 (1991).
9. J.-P. Shaw, J. A. Fishback, K. C. Cundy, and W. A. Lee. A Novel Oligonucleotide Inhibitor of Thrombin. I. *In Vitro* Metabolic Stability in Plasma and Serum. *Pharm. Res.* **12**:1937 (1995).
10. P. C. de Smidt, T. L. Doan, S. de Falco, and T. J. C. van Berkel. Association of Antsense Oligonucleotides with Lipoproteins Prolongs the Plasma Half-life and Modifies the Tissue Distribution. *Nucl. Acids. Res.* **19**:4695 (1991).
11. G. Goodarzi, M. Watabe, and K. Watabe. Organ Distribution and Stability of Phosphorothioated Oligodeoxyribonucleotides in Mice. *Biopharm. Drug Disp.* **13**:221 (1992).
12. S. Agrawal, J. Temsamani, and J. Y. Tang. Pharmacokinetics, Biodistribution, and Stability of Oligodeoxynucleotide Phosphorothioates in Mice. *Proc. Natl. Acad. Sci. USA* **88**:7595 (1991).
13. P. A. Cossum, H. Sasmor, D. Dellinger, L. Truong, L. Cummins, S. R. Owens, P. M. Markman, J. P. Shea, and S. Crooke. Disposition of the ^{14}C-Labeled Phosphorothioate Oligonucleotide, ISIS 2105, after Intravenous Administration to Rats. *J. Pharmacol. Exp. Ther.* **267**:1181 (1993).
14. H. Sands, L. J. Gorey-Feret, A. J. Cocuzza, F. W. Hobbs, D. Chidester, and G. L. Trainor. Biodistribution and Metabolism of Internally $_3$H-Labelled Oligonucleotides.I.Comparison of a Phosphodiester and a Phosphorothioate. *Mol. Pharmocol.* **45**:932 (1994).
15. H. Sands, J. Gorey-Feret, S. P. Ho, Y. Bao, A. J. Cocuzza, D. Chidester, and F. W. Hobbs. Biodistribution and Metabolism of Internally $_3$H-Labelled Oligonucleotides. II. 3',5'-Blocked Oligonucleotides. *Mol. Pharmacol.* **47**:636 (1995).
16. H. J. Gaus, S. R. Owens, M. Winniman, S. Cooper, and L. Cummins. On-Line Electrospray Mass Spectrometry of Phosphorothioate Oligonucleotide Metabolites. *Anal. Chem.* **69**:313 (1996).
17. P. A. Cossum, L. Truong, S. R. Owens, P. M. Markman, J. P. Shea, and S. Crooke. Pharmacokinetics of a ^{14}C-Labeled Phosphorothioate Oligonucleotide, ISIS 2105, after Intradermal Administration to Rats. *J. Pharmacol. Exp. Ther.* **267**:1181 (1993).
18. J. Rappaport, B. Hanss, J. B. Kopp, T. D. Copeland, L. A. Bruggeman, T. M. Coffman, and P. E. Klotman. Transport of Phosphorothioate Oligonucleotides in Kidney: Implications for Molecular Therapy. *Kid. Int.* **47**:1462 (1995).
19. R. Oberbauer, G. F. Schreiner, and T. W. Meyer. Renal Uptake of an 18-mer Phosphorothioate Oligonucleotide. *Kid. Int.* **48**:1226 (1995).